DEVELOPMENT OF A WIDELY TUNABLE ALL FIBER LASER SOURCE FOR RAMAN SPECTROSCOPY/MICROSCOPY

by

Sean Crystal

A Thesis Submitted to the Faculty of the

COLLEGE OF OPTICAL SCIENCES

In Partial Fulfillment of the Requirements

For the Degree of

MASTER OF SCIENCE

In the Graduate College

THE UNIVERSITY OF ARIZONA

2019

THE UNIVERSITY OF ARIZONA
GRADUATE COLLEGE

As members of the Master's Committee, we certify that we have rea d the thesis prepared by Sean Crystal, titled, Development of a Widely Tunable All Fiber Laser Source for Raman Spectroscopy/Microscopy and recommend that it be accepted as fulfilling the dissertation requirement for the Master's Degree.

_____ Date: 06/10/2019
Dr. Khanh K. Kieu (Committee Chair)

_____ Date: 6/10/2019
Dr. Jason Jones (Committee Member)

_____ Date: 6/10/19
Dr. Tsu-Te Judith Su (Committee Member)

Final approval and acceptance of this thesis is contingent upon the candidate's submission of the final copies of the thesis to the Graduate College.

I hereby certify that I have read this thesis prepared under my direction and recommend that it be accepted as fulfilling the Master's requirement.

_Khanh Kieu_____ Date: 06/10/2019
Dr. Khanh K. Kieu
Master's Thesis Committee Chair
College of Optical Sciences

Table of Contents

I List of Figures

II Abstract

Raman microscopy is an important tool for a variety of applications, but the current laser sources used for this technology make the availability of these systems uncommon. Current laser sources are simply too complicated and expensive, taking up the footprint of an entire optics table and costing up to $500,000. There is a strong need for a simpler laser architecture which can still meet the resolution and tunability requirements of current systems. In this thesis, I describe the progress made toward developing such a laser source in the Ultrafast Fiber Lasers and Non-Linear Optics group and the College of Optical Sciences. We demonstrate promising performance results and identify areas of improvement that will soon enable our group to have a high performing Raman microscope.

III Introduction

III.I Motivation

The ability to identify specific molecules and molecular compounds is important for a variety of applications from biological microscopy to directed energy remote sensing. There are a multitude of different methods to effectively accomplish this, many of which utilize optical systems. Of the many optical methods, which include absorption spectroscopy, Fourier Transform Infrared Spectroscopy (FTIR) or dual comb spectroscopy, Raman spectroscopy has many advantages and will be the focus of this thesis.

Raman spectroscopy allows for highly accurate identification of many molecules with by use of excitation light sources in the Short-Wave Infrared (SWIR) wavelengths. Several of these types of sources are well developed, giving it an advantage over mid-Infrared (MIR) spectroscopy techniques. Additionally, Raman spectroscopy can allow for very high resolution and differentiation of molecules without the computer deconvolution operation which is needed for broadband frequency comb sources.

Our research group currently has multiple multi-photon microscopes that have been used to collect a significant amount of data from a variety of different samples. Such data has been useful for biological imaging, medical innovations and even insight into the structure of gemstones [1] [2].While our current lasers enable such information to be attained with two and three photon non-linear optical processes, the subject of this work will be on the development of an additional laser source. This laser source's multiple wavelength output, broad tuning and all fiber format will lead to more versatility in our microscope setups.

While there are existing laser sources that can be used for Raman microscopy, they suffer from high complexity and cost. These sources are, traditionally, based on bulk Titanium-Sapphire (Ti:S) lasers. While these are robust and proven laser sources, there complexity to run and high cost has limited the ability of researchers to utilize this extremely desirable tool. A versatile, cost effective and simple laser source would open the doors for new applications, research and innovation.

III.II Objective

The goal of this work is to develop a cost-effective all-fiber laser source to provide researchers and scientists with an attainable instrument to fully take advantage of such an innovative spectroscopic/microscopic technique. We will show that an all fiber Ytterbium pumped OPO not only offers simplicity compared to that of Ti:S based systems but can provide greater tunability with comparable resolution. Additionally, we aim to demonstrate Raman excitation at longer IR wavelengths than previously demonstrated, enabled by this novel source, which may allow deeper imaging capability into biological tissue.

IV Literature Review

IV.I Principles of Raman Microscopy

There are a multitude of different non-linear microscopic processes, such as multiphoton microscopy, which provide valuable data that cannot be attained from standard light microscopy. Raman microscopy is a special type of non-linear microscopy which generates microscope images of samples where the data represents, not only structural information, but also identification of chemical origin of molecules. The ability to label molecules is important for a variety of applications, especially in the biomedical field. Raman microscopy is based on the $\chi^{(3)}$ nonlinear principle of Raman Scattering. This is an inelastic scattering process based on the natural vibrational mode of any given molecule. In this process, an absorbed photon is re-emitted as a lower energy photon, known as the scattered photon. The difference of these two photons directly corresponds to the ground state vibrational mode of the molecule. Molecular vibrational modes range from 10^{12} Hz to 10^{14} Hz [3]. It happens that this difference in frequency can be accessed with optical regime electro-magnetic radiation. This is a powerful point because nonlinear processes are intensity dependent and lasers developed in this spectral regime provide a great source to meet these intensity demands.

There are many types of Raman processes but, for the purpose of microscopy, the focus will be on Stimulated Raman Scattering (SRS) and Coherent Anti-Stokes Raman Scattering (CARS). The Raman scattering process can lead to two different wavelength shifts, stokes and anti-stokes. A stokes shift refers to the case where the material gains energy from the interacting photon and emits a lower frequency photon. An anti-stokes shift occurs when the material losses energy to the interacting photon and emits a higher frequency photon [3]. SRS is generally based on the first case and CARS on the latter. Both SRS and CARS are accomplished by using two overlapping laser wavelengths to excite the molecules ground state vibrational mode, or shift. Equation 1), shows the relation between the pump wavelength, scattered wavelength and the shift.

$$1)\ \frac{1}{\lambda_{Pump}} - \frac{1}{\lambda_{Scatter}} = Shift$$

If the molecular shift is known, the two laser wavelengths can be tuned to match the shift with this equation. At large enough intensities this will induce a stimulated process which can be observed, thereby a significant improvement conversion efficiency can be observed.

The SRS energy level diagram is shown in Figure 1. The orange arrow represents a pump photon and the red arrow represents the Stokes photon. It can be seen from this energy

diagram that in this process, the difference of their two energies equal that of the vibrational mode. In practice this is done with two high peak power ultra-short laser pulses (usually on the order of pico-seconds). By overlapping these two pulses, both in space and time, and focusing them down onto a sample, the SRS process can be induced. In a microscope set up, these two pulses are scanned with two steering mirrors and focused by an objective lens. Traditionally, an intensity modulation is applied to the pump arm and when the vibrational mode of a molecule is met the modulation is transferred to the stokes arm. When this modulation is detected at a specific point, the image formed by the microscope will possess a Raman indicative signal at the correlating pixel.

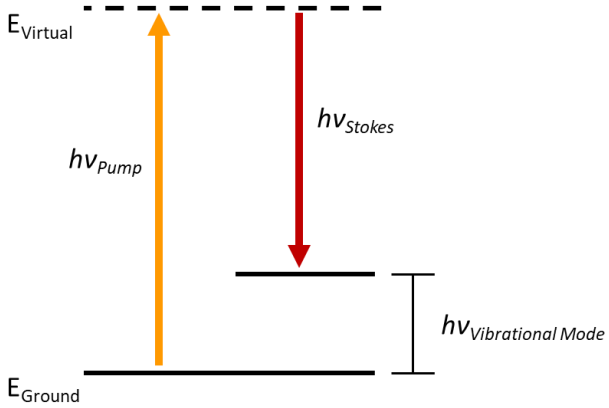

Figure 1: Virtual energy diagram of CARS.

The CARS energy level diagram is shown in Figure 1. This process is slightly more complicated than SRS but is more straightforward to detect. As seen in the energy diagram, a pump and stokes photon excite the vibrational mode of the molecule. A second pump photon, referred to as the probe photon, then excites the molecule to a higher virtual state where it decays as a blue shifted (anti-Stokes) photon, shown as the green arrow. In practice this process is induced very similarly to that of SRS, with two overlapped pico-second pulses directed onto a microscope sample with two steering mirrors and an objective lens. The difference is that a blue shifted photon is emitted. This means that no modulation transfer needs to be detected and, instead, the higher frequency photon can be split off and detected directly. When this blue shift is detected, the image formed by the microscope will possess a Raman indicative signal at the correlating pixel. The drawback of CARS is that it has a non-resonant background whereas this unwanted background is effectively removed in SRS mode.

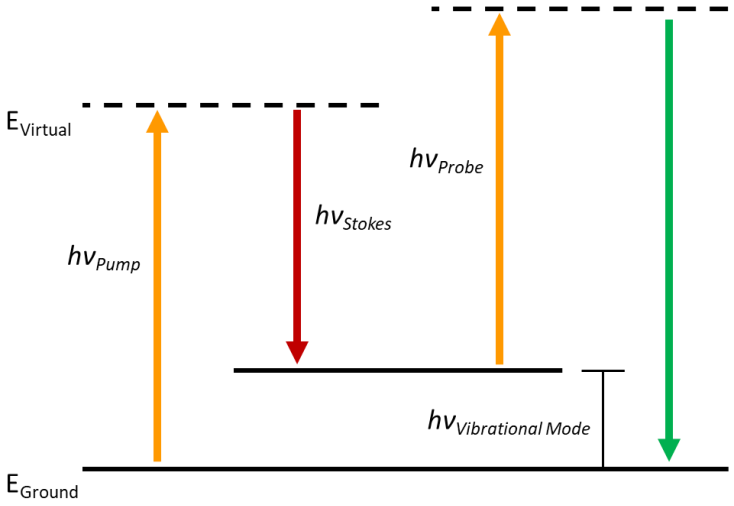

Figure 2: Virtual energy diagram of SRS.

These processes are essentially a type of spectroscopy that, when paired with a microscope, provide both spectroscopic and spatial data. Because Raman is a non-linear process, it possesses unique characteristics that make it interesting for microscopy. This includes the fact that imaging can occur with no stains and that 3D information can be gathered because this excitation only occurs at the focus.

Significant research has been done in developing sources for this microscopy technique. Ytterbium pumped free space Optical Parametric Oscillator (OPO) have been developed for pump and stokes photon excitation by Hanninen [4] and Kieu et al [5]. These systems showed high spectral resolution but limited tunability and were also bulky and expensive. A commercial Titanium Sapphire (Ti:S) pumped OPO was utilized by Ito et al [6] to produce Raman images, but this system was very limited in both tuning and resolution. Ti:S locked with Ytterbium lasers have been demonstrated by ozeki Et al [7] [8]. While the system in these papers had very high spectral resolution, they were also significantly limited in their tunability. A few fiber based OPO sources have been demonstrated by Lamb et al [9], Lefrancois et al [10], and Gottschall et al [11]. These fiber OPO based lasers show some of the greatest spectral resolution but, again, very limited tunability. The specifications of these papers are summarized in Table 1. It can be seen that a system with both high spatial resolution and broad tunability that is constructed in a simple and cost-effective format has yet to be successfully developed.

1st Author	Device	Tuning (cm^{-1})	Resolution (cm^{-1})
Ozeki Et al	Custom tunable Yb laser and Ti:S	2800-3100	3
Hanninen	Commercial Yb laser and OPO	2800-3020	10
Ozeki Et al	Custom tunable Yb laser and Ti:Sa	2800-3100	3
Gambetta et al	Single laser, Commerical Er and PPLN doubling	1000-3000	<15

Kieu et al	Custom Yb fiber laser, OPO pumped for tunable CARS	Signal tuned from 740-1005	.9
Ito et al	Commericial Ti: Sa	400-1000	25
Brinkmann Et al	FOPO pumped by commercial 1030 laser	860-2075	21
Lamb et al	Yb fiber laser pumping FOPO for Cars (free space)	2740-3150	4.6
Gottschall et al	Yb fiber laser pumps FOPO, uses free space optics	2800-2970	1

Table 1: Summary of relevant current literature that have shown development of laser sources or Raman microscopy and there specifications.

IV.II Review of Ultrafast Fiber Laser's

Ultra-fast laser sources are extremely important for a variety of applications ranging from material processing to directed energy. What is unique about these systems is that they can produce extremely high peak powers in very short time scales. Unfortunately, these systems are typically large, bulky and very expensive. For example, Ti:S laser systems can produce sub-20fs pulses with Terra-watts of peak power but may cost on the order of $500,000 and have the footprint of an entire optical bench.

Ultra-fast fiber lasers offer a more compact, rugged and cost-effective solution to the previously mentioned systems. Instead of parts mounted to optical breadboards, fine-tuned mirrors and bulk crystals, fiber lasers can be made with all fiber components such as Wavelength-Division Multiplexers (WDM's) for combining pumps, fiber optic couplers for outcoupling and doped gain fiber as a lasing medium. These components are spliced together, and the light is confined inside the guiding core. Another benefit of fiber lasers is their high beam quality.

Depending on the system, they can show interesting characteristics in their dispersion and non-linear optical properties which provide benefit, but can also add complexity. For instance, the high dispersion can be used to make simple pulse stretchers and compressors without grating pairs, but this can also lead to undesired pulse dynamics in oscillators such as mode-pulling. Non-linear effects are usually dependent on intensity and interaction length, therefore, the small confinement inside fiber and the ability to coil kilometers of fiber on a small spool make these effects prominent in such systems. The non-linear properties are often taken advantage of, as is done in this thesis, but can also cause undesired effects that reduce power or create instabilities.

Fiber optic lasers typically operate in 1μm, 1.5μm or 2μm spectral range due to the rare earth ion dopants commonly doped in silica fiber, Ytterbium, Erbium and Thulium. There are some other dopants and host materials, but these are the most common. Mode-locking of these systems are typically accomplished by use of a Saturable Absorbing Mirror (SAM), which is a semiconductor grown atop a small mirror substrate, butt coupled to the end of a fiber or by use of carbon nano-tubes and fiber tapers in-line with the fiber. Such

mode-locking mechanisms are capable of producing pico-second and femto-second time scale pulses with mega-hertz repetition rates.
Figure 3 shows a schematic example of a typical mode-locked ultra-fast fiber laser. It is pumped by a CW, narrow linewidth, fiber coupled laser diode. This light is coupled into the cavity through use of a Fiber Bragg Grating (FBG), which is a fiber with periods of alternating refractive indices, written in by UV lasers and phase masks, which transmit and reflect certain amounts of specific wavelengths. This device is also used as the out-coupler. A rare-earth doped gain fiber is typically used as the lasing medium and a SAM is used as the second end of the cavity plus the mode-locking mechanism. These components are usually low cost and simple to be spliced together. It should be noted that this is one example of an ultra-fast fiber laser and there are many other configurations.

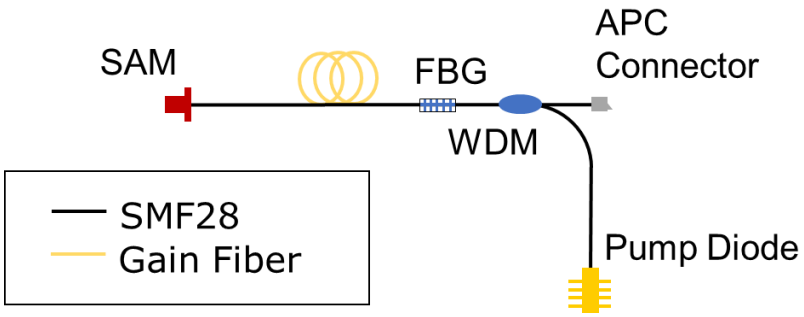

Figure 3: Schematic of typical mode-locked ultra-fast fiber laser.

IV.III Non-linear Parametric Processes and FOPO

Parametric non-linearities are instantaneous optical wavelength conversion/amplification processes that occur in $\chi^{(2)}$ and $\chi^{(3)}$ nonlinear materials. In a standard laser gain medium, an electron of an atom is excited with a certain frequency pump photon and a lower frequency photon is emitted with some amount of gain. Parametric processes are very different. In these processes, the quantum state of the electron does not change, and the pump photon energy is directly transferred to a wavelength shifted photon. The role of the non-linear medium in this process is to phase match the interacting waves.
There are many parametric processes including frequency doubling/tripling, sum/difference frequency generation, four-wave-mixing and optical parametric oscillation/amplification [12]. The laser described in this thesis utilizes the process of four-wave-mixing and optical parametric oscillation. This will now be further described.

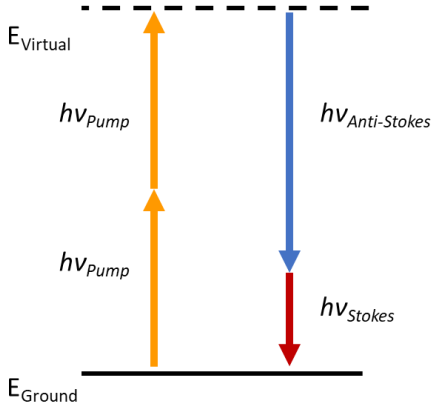

Figure 4: Virtual energy level diagram of the four-wave-mixing process

The four-wave-mixing process is based on $\chi^{(3)}$ nonlinearity. This process involves four photons, hence the name. Figure 4 show the energy level diagram where two pump photons excite a virtual energy state. The decay from this state results in one anti-Stokes (blue shifted) and one Stokes (red-shifted) photon. This process requires proper phase matching of the wavevectors which is described by equation 2) [13]:

$$2)\ \Delta k = 2k_0 - k_1 - k_{-1}$$

By placing a $\chi^{(3)}$ material inside a resonator, properly phase matching and pumping it hard enough, the pump photon energy will be transferred to the Stokes and anti-Stokes photon. This is known as a $\chi^{(3)}$ based Optical Parametric Oscillator (OPO). This is the type of OPO which can be made in an all fiber format because fused silica, which is what most fiber is made from, has a $\chi^{(3)}$ nonlinearity.

The advantage of this parametric process is that the generated frequencies are not dependent on intrinsic crystals' energy bands, but purely on whether the interacting frequencies can be phase matched. This enables gain over a wide spectral range which cannot be accomplished with naturally occurring laser gain materials. Depending on the application, the signal and/or idler can be used.

V Laser System Development

The development of our all fiber laser system is a key element to enabling this simplified Raman spectroscopy/microscopy device. The general concept of this laser is to generate two wavelengths from one single source which can then be combined for Raman excitation. The work discussed below is built upon previous work done within our group. Multiple design considerations had to be considered to make this specific system well suited for Raman microscopy.

The laser system is divided up into four main parts: The mode-locked Ytterbium oscillator, a series of Ytterbium amplifiers, a secondary Ytterbium amplifier, and finally a Fiber Optical Parametric Oscillator (FOPO) for generation of the anti-stokes wavelength. Figure 5 shows the schematic diagram of the full system, identifying the four segments that will be discussed in detail.

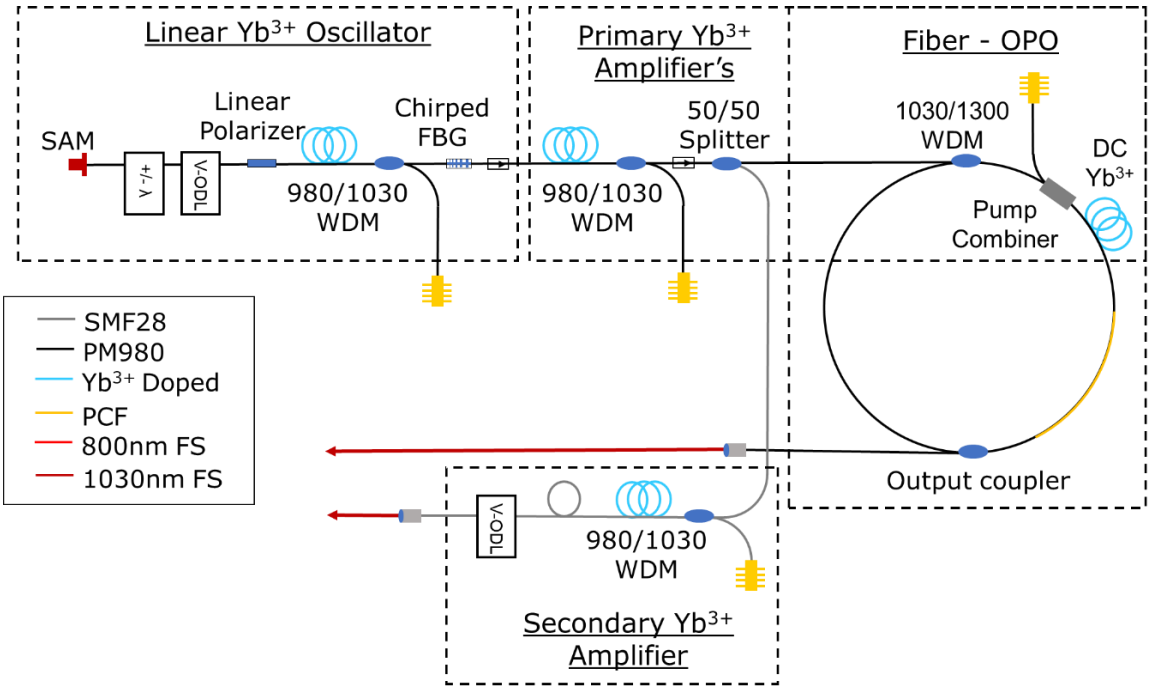

Figure 5: Full schematic of the two wavelength Raman microscopy laser constructed. The system is comprised of an Ytterbium oscillator, set of YDFA's and a FOPO.

V.I Mode-Locked Ytterbium Fiber Oscillator

V.I.I Description

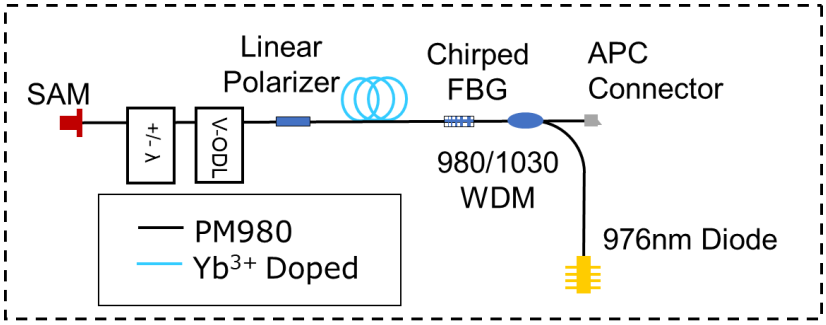

Figure 6: Schematic of the linear, mode-locked all PM Ytterbium fiber oscillator.

The front end of this entire laser system is that of the diode pumped linear mode-locked fiber oscillator as seen in Figure 6. This oscillator provides the original low power 1µm seed which will be used throughout the rest of the system.

Figure 6 shows the schematic of the mode-locked Ytterbium oscillator producing the 1µm seed for this system. This is a low power oscillator which produces both temporally and spatially clean picosecond duration, megahertz repetition rate pulses.

A 796 nm fiber coupled and wavelength stabilized laser diode controlled by a Wavelength Electronics driver acts as the optical pump source for the oscillator. It is coupled into the cavity through a 980nm/1030nm wavelength division multiplexer (WDM) and a broadband 50% reflective Fiber Bragg Grating (FBG). The FBG acts as the outcouple for the cavity, while the WDM directs pump light into the cavity and the outcoupled light to the next stage of the system.

The laser oscillator is mode-locked by a Saturable Absorbing Mirror (SAM) from BATOP Optoelectronics. This device is comprised of a small semi-conductor grown atop of a mirror substrate. This is butt coupled to the end of a flat fiber connector with index matching gel, while a second flat fiber connector is used to apply pressure for good contact. Many different SAMs were tested in this system to find one working in the desired spectral tuning range and with the right response time.
The gain mechanism in this cavity is comprised of 60cm of Ytterbium doped gain fiber purchased from CoreActive. This fiber has a peak absorption around 980nm and emission between 1020nm – 1055nm. Because the emitted 1µm light is not polarized while the rest of the cavity is Polarization Maintaining (PM), a fiber coupled linear polarizer is inserted into the cavity after the gain fiber. This Ytterbium fiber has very high gain, so long segments of gain fiber are not necessary.
There are two other important components in this cavity. First, the wavelength tuner is a fiber coupled bandpass filter purchased from Agiltron Inc. which allows central wavelength tunability of the oscillator. This is the main Raman response tuning mechanism for the entire system. The second component is the delay line. The delay line allows cavity length tunability (thereby its repetition rate tunability) which helps in synchronously pumping the FOPO.

V.I.II Characterization

The pump diode, purchased from 3S photonics, was characterized to confirm manufacturer specified performance before integration into the oscillator. The Light/Current (LI) curve can be seen in Figure 7. The shape is linear, as expected, and an output of 589.5mW can be attained with 912.5mA of current. This output power is more than enough to pump the oscillator and the first primary amplifier stage. The spectrum can be seen in Figure 7. It is centered at 975.6nm and has a linewidth of 0.4nm at -3dB.

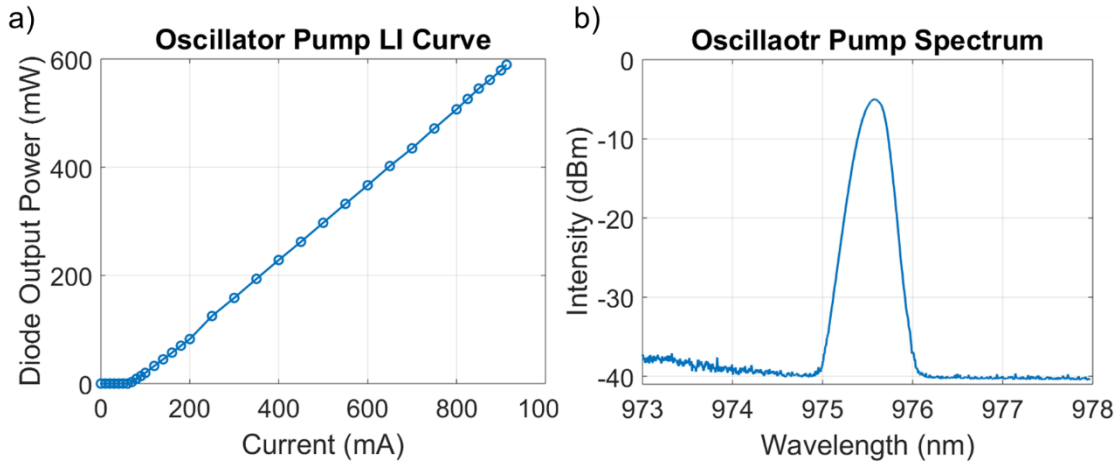

Figure 7: a) The Light/Current curve of the pump diode. b) The pump diode emission spectrum.

The mode-locked oscillator spectrum can be seen in Figure 8. This data was gathered from an Anritsu OSA. Figure 8a) shows a zoomed in spectrum centered at 1039nm. The mode-locked laser spectrum has a -3dB linewidth of .3nm - .4nm. Figure 8b) also shows the tuned mode-locked laser spectrum. Tunability was achieved from 1026nm to 1052nm while still maintaining stable mode-locking.

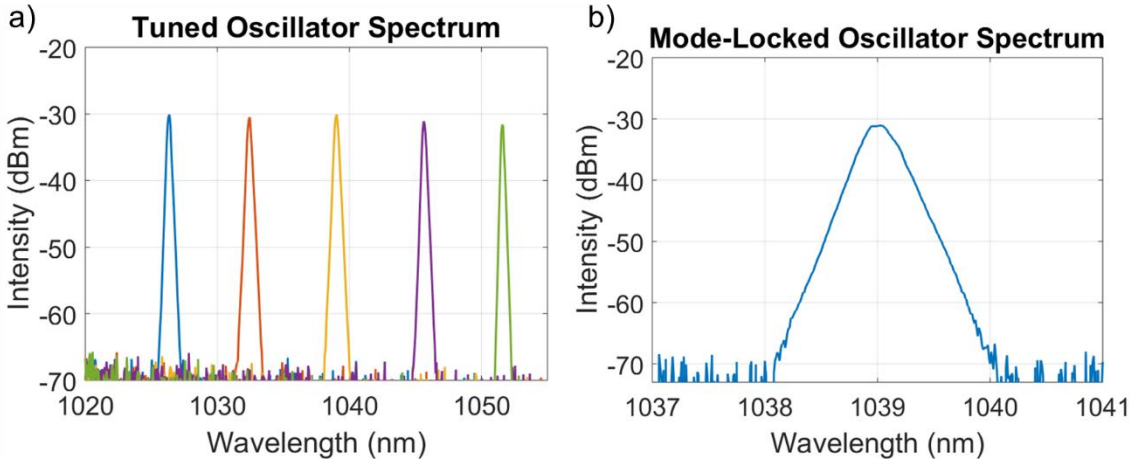

Figure 8: a) Zoomed in spectrum of the laser after mode-locking at 1043nm displaying the expected triangular shape. b) Multiple mode-locked spectral peaks tuned from 1026nm to 1052nm.

In order to characterize the pulse dynamics, a 100MHz fast photo-diode, 500MHz oscilloscope, and GHz frequency spectrum analyzer were utilized. Figure 9a) shows the pulse train from the oscillator while Figure 9b) shows a single peak at the repetition rate of the laser. The repetition rate, measured in both the time and frequency domain, was found to be 21.67MHz, corresponding to a cavity length of ~9.48m (assuming a constant n=1.46 refractive index throughout the fiber cavity).

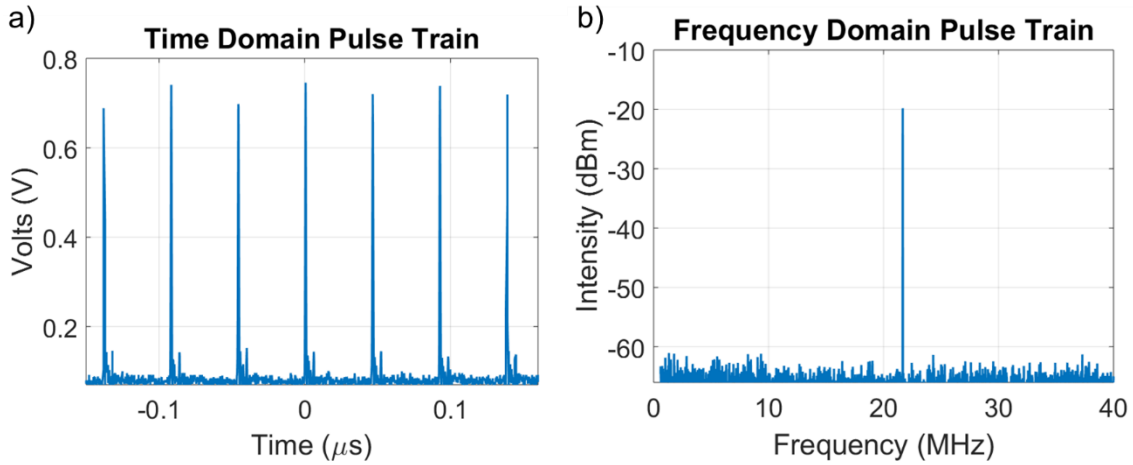

Figure 9: a) Oscilloscope trace of the oscillator pulse train. b) Frequency spectrum analyzer of the pulse train showing a rep-rate of 21.67MHz.

The current oscillator is only self-starting in the double pulsing regime. For this reason, starting the oscillator is achieved by increasing the pump diode current until double pulsing occurs, then lowering the current until the single pulsing regime is achieved. From this regime, the following data in Table 2 was collected. Continuous wave (CW) operation was achieved at 42.5mW input pump power. The upper pump threshold was found to be ~72.0mW and the oscillator would stay mode-locked after lowering the power down to ~54.0mW due to hysteresis. After much experimenting, it was determined that the oscillator ran most stable with at a pump power of ~62.2mW. The oscillator would stay stably mode-locked for >10 hours at this running point.

	CW	Lower ML	Upper ML	Run Point

Controller Volts (V)	.273	.310	.375	.342
Input Power (mW)	42.5	54.0	72.0	62.2
Output Power (mW)	.04	.9	1.3	1.2

Table 2: Characterization of the pump diode voltages, power and oscillator power for various oscillator running regimes.

V.II Primary Ytterbium Fiber Amplifiers

V.II.I Description

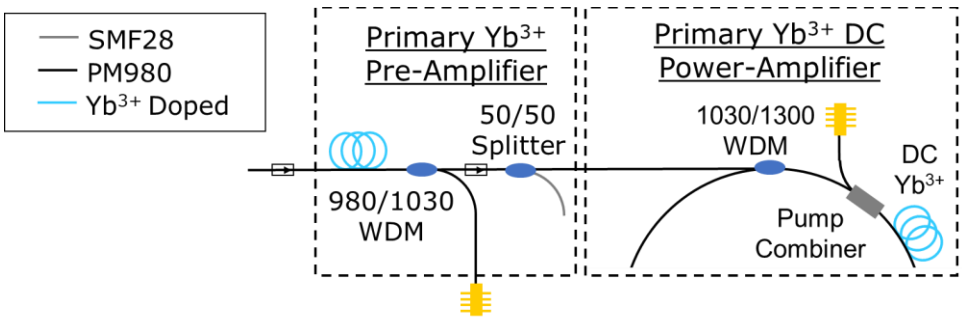

Figure 10: Schematic of the primary Ytterbium fiber amplifiers chain including the splitting of the signal for the secondary Ytterbium amplifier.

In order to properly seed the FOPO, the low power 1µm oscillator signal must be amplified. Not only is there a threshold to the parametric gain, but a certain amount of Stokes light must be generated to excite the Raman response of our sample. Two stages of Ytterbium fiber amplifiers (YDFA) are implemented to accomplish this. The first stage is a counter pumped pre-amplifier and the second stage is a co-pumped high-power double-clad amplifier. Figure 10 shows the schematic of the amplifiers.

The first stage pre-amplifier is pumped by a second 976nm fiber coupled and wavelength stabilized diode. This diode is wired to a Newport 8000 Diode controller to run the drive current and Thermo Electric Cooler (TEC). In the final packaged system, this diode will not be needed, as a portion of the power from the oscillator pump will be split off to pump this pre-amplifier. The current pump was characterized up to 400mA of drive current, corresponding to 208mW of pump power. The rest of the amplifier is comprised of Ytterbium gain fiber and a 1064nm isolator to prevent any reverse propagating signals from disturbing the oscillator.

50% of the signal from the pre-amplifier is split off and sent to the secondary Ytterbium amplifier, the reason for this will be explained further in the corresponding section. The remaining 50% was sent to the power amplifier. This seed travels through a 1030nm/1300nm WDM which is part of the FOPO ring cavity, then a high-power pump combiner is used to combine the pre-amplifier seed and the high-power, multi-mode fiber coupled pump diode. This pump diode is wired to the second channel of the Newport 8000 Diode controller. This diode can provide up to 9W of output power. For the purposes of this system, it was characterized up to a 4.8A drive current with a corresponding output power of 2.76W, more than enough to amplify our seed for the FOPO.

The resulting power and spectral broadening are the two key factors that must be considered while constructing these amplifiers in order to have an efficient and powerful

enough FOPO. Custom made high-efficiency large mode area double clad Ytterbium gain fiber was used as the gain medium for high-power amplification with these factors in mind. Double-clad (DC) gain fiber allows for high power pump light to be coupled into the core and first cladding. The seed propagates in the core but sees gain from all the excited ions in the core and first cladding. Originally, 1.1m of this gain fiber was used. This led to an efficiently working amplifier, but, unfortunately, the large length of gain fiber led to significant Self Phase Modulation (SPM) and therefore significant spectral broadening. Because we wish to run this FOPO narrow-band, this broadened seed causes problems with both the resulting bandwidth of the idler and the efficiency of parametric conversion. In order to reduce the SPM, the length of the DC gain fiber was reduced. While this decreased the efficiency of the amplifier, it reduced the SPM by nearly half. Because this is a low power FOPO system, we are willing to sacrifice the amplifiers efficiency for a less broadened spectrum. The original amplifier was constructed outside the FOPO cavity, but after realization that any length of fiber the amplified seed traveled through would add to the accumulated SPM, the high-power amplifier was moved into the FOPO cavity so that the narrowest possible amplified signal would see the parametric gain fiber. It should also be noted that because the core of the gain fiber is 10μm in diameter and that of the rest of the fiber in the cavity is 6μm, a fiber bridge must be constructed to get efficient power throughput to the PCF. This particular bridge was constructed by splicing a 1cm length 8.5 μm in-between the gain fiber and the next piece of PM980.

V.II.II Characterization

The power and spectral characterization of the pre-amplifier can be seen in Figure 11. Nearly 40mW of output power from 200mW of input power could be achieved. The slope efficiency of this amplifier was found to be only 24%. This low efficiency is suspected to be because the seed from the oscillator passes through a 1064nm isolator. The specifications for this isolator show it has high loss outside 1059nm – 1069nm. Due to this, it is believed that the pre-amplifier is not fully saturated and that the replacement of this component with a broadband isolator would fix this problem. In addition to the amplifier's inefficiency, it should also be noted that the amplified signal passes through a second 1064nm isolator after the amplifier where an additional 40% loss occurs.
Along with the power, the spectral characteristics of the pre-amplifier were also evaluated. It can be seen in Figure 11b) that very little spectral broadening was observed after amplification. Even at the greatest pumping power the spectrum expanded only to 0.62nm at -3dB.

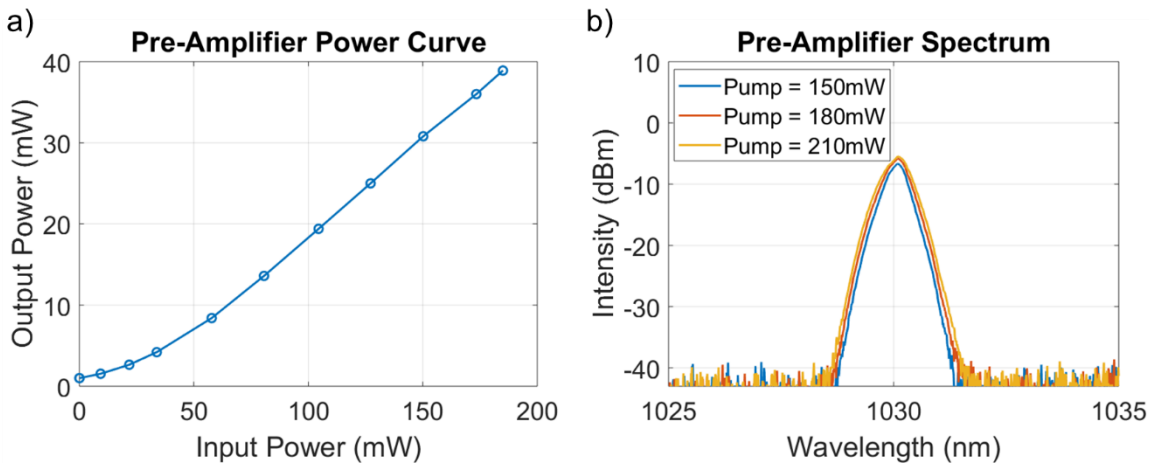

Figure 11: a) Input-Output characterization of the primary pre-amplifier. b) Spectral characterization of the primary pre-amplifier for varying pump powers.

After passing through the isolator, the pre-amplifier output is sent through a 50/50 coupler where ~10mW is output from each arm. One arm is passed through the FOPO WDM and pump combiner where ~9mW of signal remains to and is seeded into the power-amplifier. This is enough to saturate the DC-YDFA.

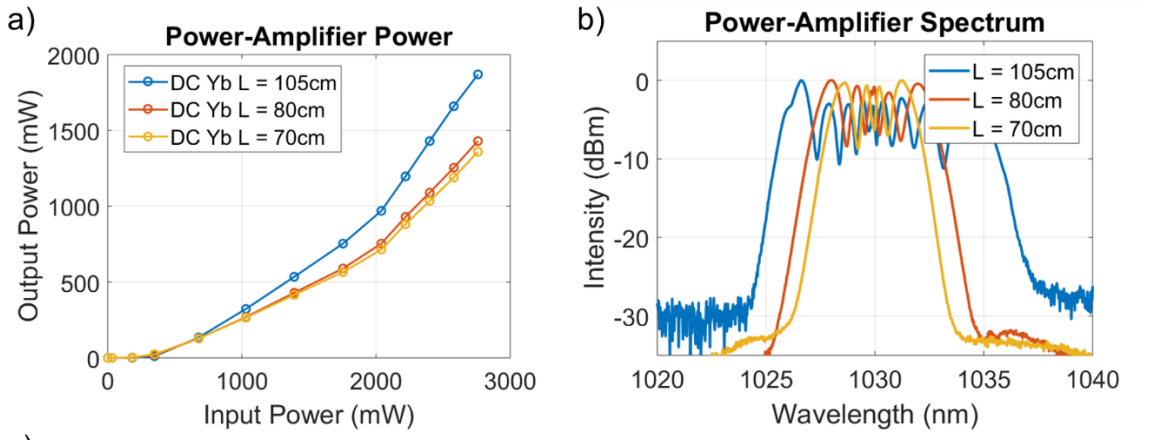

c)

DC Yb Length (cm)	Slope Efficiency (%)	Overall Efficiency (%)	Linewidth (nm)
105	82.6	67.8	8.5
80	61.6	51.8	6.2
70	58	49.3	4.15

Figure 12: Characteristics of the power amplifier at varying gain fiber lengths a) Input-Output curves. b) Spectra. c) Table summarizing efficiencies and linewidths.

As mentioned in the prior section, the power-amplifier was originally constructed with 1.1m of DC Ytterbium gain fiber. While this resulted in a very respectable slope efficiency of 82.6%, SPM in this length of fiber resulted in a linewidth of 8.5nm. In order to reduce the linewidth, the amplifier gain fiber length was cut back from 105cm to 80cm and finally to 70cm. The resulting power curves and spectra are shown in Figure 12. While reducing the gain fiber length reduced the slope efficiency from 82.6% to 58%, it also reduced the linewidth from 8.5nm to 4.15nm. Because the goal of this FOPO is not a

high-power output, we are willing to sacrifice some efficiency for a narrower spectrum. There is of course a limit set by the parametric gain threshold and the desired output power in the idler. By reducing the gain fiber length to 70cm, the spectral linewidth is reduced by nearly half it was at 105cm, while still providing more than 1W of output power, which should still be enough.

V.III Secondary Ytterbium Fiber Amplifier:

V.III.I Description

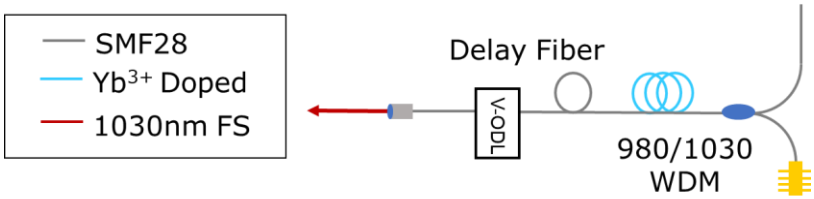

Figure 13: Schematic of the secondary Ytterbium fiber amplifier.

The first of two wavelengths produced from this laser source to induce Raman excitation in the microscope samples is that of the 1µm seed. While the resulting FOPO will output residual 1µm pump light, this signal is broader than desired and may drift off, in time, from the 1.3µm stokes signal. For both reasons, a portion of the 1µm seed is split off before the FOPO cavity and re-amplified in a secondary YDFA. This signal is then precisely delayed to over-lap in time with the generated 1.3µm stokes signal.
The secondary pre-amplifier is non-PM, comprised of Lucent-980 fiber and CoreActive Yb-402 gain fiber. It is co-pumped by a 976nm diode. After amplification, the amplified signal is delayed, in order to overlap with the FOPO generated stokes signal.

V.III.II Characterization

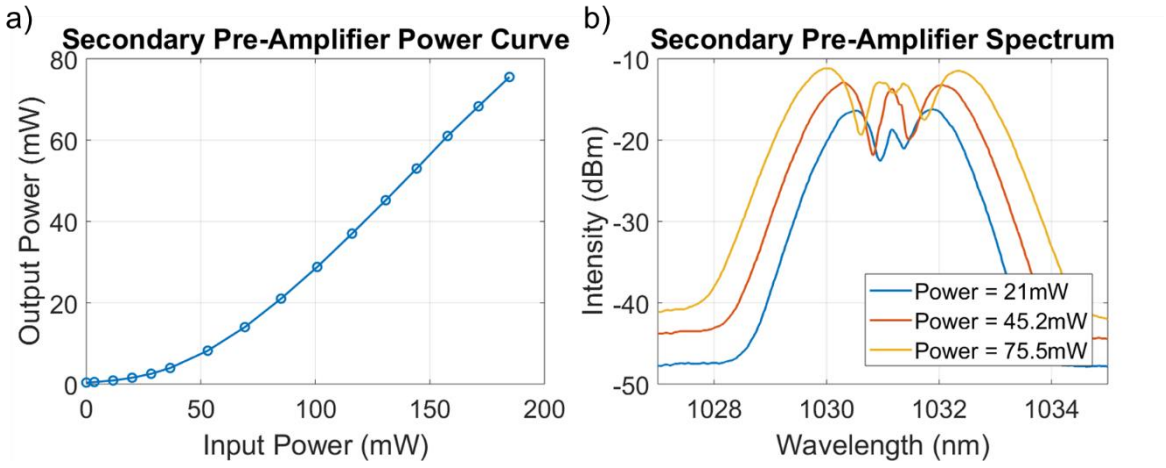

Figure 14: Input-Output characterization of the secondary pre-amplifier. b) Spectral characterization of the secondary pre-amplifier for varying pump powers.

The secondary pre-amplifier power and spectral characteristics are displayed in Figure 14. 75mW of 1µm signal was generated from 185mW of pump power, corresponding to a slope efficiency of 54.2%. The 75mW signal has a linewidth of 3.3nm. This linewidth will work well for high resolution of the induced Raman response.

V.IV All Fiber Optical Parametric Oscillator

V.IV.I Description

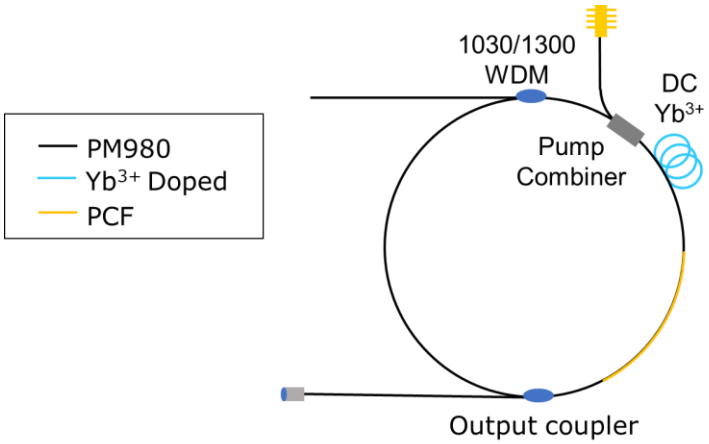

Figure 15: Schematic of FOPO including the high-power YDFA incorporated within the cavity.

The all fiber Optical Parametric Oscillator is the wavelength conversion mechanism of this laser system which is used to generate the second signal for Raman excitation. This oscillator will generate a blue shifted signal and a red shifted idler. For this Raman microscopy project, we take advantage of the idler which will be re-combined with the secondary amplified 1µm pump. The 1µm secondary pump and the 0.8µm signal can also be used for Raman or other multi-photon applications.

This OPO takes advantage of the χ^3 nonlinearity of fiber. In order to generate a good FOPO, a fiber with zero dispersion near the pump wavelength must be used. No standard fibers exist which have this property, so dispersion engineered, Photonic Crystal Fiber (PCF) is used as the phase matching mechanism requires. The oscillator itself is an all fiber ring cavity made from the power amplifier, PCF, output coupler, WDM and meters of PM980. The schematic of this oscillator can be seen in Figure 15.

V.IV.II Simulation

The LMA5-PM PCF is well characterized by [14]. A MATLAB program, which was written by our group, based on this paper was utilized to determine the phase matching conditions and gain curves of this system. The relevant equations, which describe this, are as follows:

$$3)\ \Omega(\omega_p) = \left(\frac{-P(\omega_p)}{2} + \sqrt{\left(\frac{-P(\omega_p)}{2}\right)^2 - \frac{-24\gamma P_p}{\beta_4}}\right)^{1/2}$$

$$4)\ P(\omega_p) = 12\,\frac{\beta_3}{\beta_4}\,(\omega_p - \omega_0) + 6\,(\omega_p - \omega_0)^2$$

Where Ω is the parametric frequency shift, P_p is the pump power, β_3 and β_4 are the 3rd and 4th order dispersion, ω_p the pump frequency and ω_0 is the zero-dispersion frequency of the parametric gain fiber.

It can be seen from these equations that the gain is affected primarily by the pump power, pump wavelength and $3^{rd}/4^{th}$ order dispersion. The wavelength and power are used to tune that output, as the dispersion of the PCF is set. The phase matching and gain curves can be seen in Figure 16.

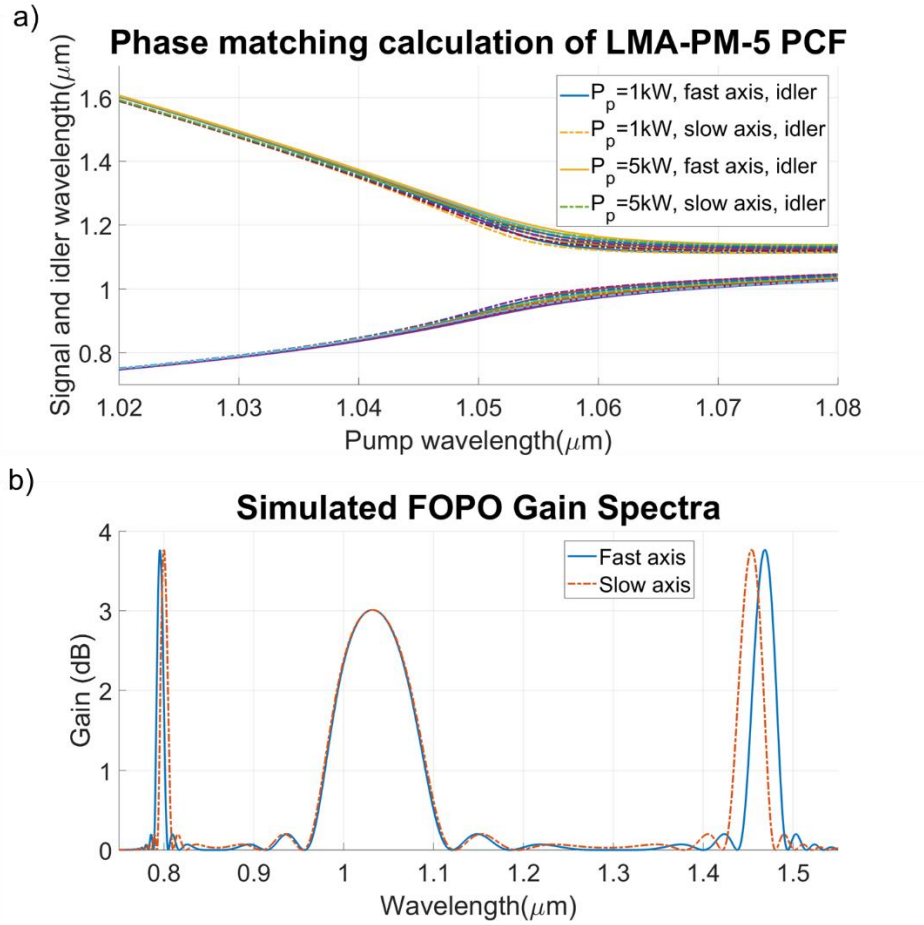

Figure 16: a) Phase matching curves for LMA5-PM PCF for varying pump wavelength and power. b) The simulate gain curves for the signal and idler with a 1032nm pump.

Figure 16 a) shows the phase matching curves for LMA5-PM PCF with a 1032nm pump. The desired idler wavelengths we are looking for in this system, 1.3µm -1.5µm, are mainly affected by pump wavelength as opposed to the pump power. Therefore, pump wavelength is the primary tuning mechanism. The gain curves shown in Figure 16 b) confirm that there will be significant gain for our desired wavelengths.

V.IV.III Construction

For this FOPO, LMA-PM5 PCF, from NKT photonics, was the specific PCF used. The rest of the cavity is comprised primarily of PM980 and some PM1550. The overall dispersion of this cavity is normal.

Both signal and idler resonant OPO configurations were constructed, by changing the WDM from a 1030nm/800nm to 1030nm/1300nm. It was shown that idler resonate FOPO's generated a narrower band signal and idler. This is commensurate with the results of previous work in our group. We desire narrow band spectra for high resolution Raman microscopy. It should also be noted from **Error! Reference source not found.**,

that the primary power amplifier was located inside the FOPO cavity. This configuration was chosen for two reasons. First, little attenuation occurred between the amplifier and the phase matching medium. Second, this limits SPM that is added to the amplified 1μm pump, thereby reducing spectral broadening, before the phase matching medium. The pumps narrow spectral width is important to the efficiency and narrow linewidth of the generated signal and idler.

Multiple out-couplers were also tested. The FOPO is a relatively high gain system and it was determined that larger out-coupling, low feedback was best. A custom out-coupler designed to have an out-coupling ratio of 90/10 at 1300nm was finally used.

The length of this cavity is very important and extremely sensitive. The round-trip time of the resonating pulse in the OPO must be the same as that of the Yb oscillator. By doing this only one pulse is in the cavity at a time and the resonating pulse perfectly overlaps with the next input pulse. This scheme is referred to as synchronous pumping and is a key requirement of OPO. The repetition rate of the oscillator was previously shown to be ~21.67MHz, this corresponds to 9.48m assuming a constant refractive index of 1.46. The delay line in the oscillator is capable of adjusting the cavity length by ± 5cm. This is not a significant amount of freedom with 9.48m of fiber. In order to accurately match the cavity lengths, the following electrical/time domain observation approach was taken.

1) The filter based micro-optics WDM in the FOPO was replaced with any fused based fiber component (Couplers work well). This was done to allow the 1μm pump signal to propagate.
2) The output of the FOPO was coupled to a highly-sensitive photo-diode connected to 1 port of a fast sampling oscilloscope.
3) A tap from the oscillator was sent to a second photo-diode which is connected to the trigger port of the same fast sampling oscilloscope.
4) The FOPO cavity length was set to a few meters less than the expected length. By doing this one can observe the oscillator pulse and the FOPO resonant pulse separated in time on the oscilloscope.
5) From here small amounts of fiber were spliced into the cavity and the change in pulse separation was noted each time to build up confidence in the electrical observation corresponding to the actual added fiber.
6) Once the difference between the oscillator and FOPO resonate pulse were less than 1m in fiber length, the fused based fiber component was removed, and the filter-based WDM was re-inserted with fiber lengths equal to that of the removed fused component plus the last difference in fiber length measured on the oscilloscope. Special accommodation should also be taken for the loss in fiber that will come from the cleaves made to splice this component into the cavity.

The synchronously pumped scheme described previously is a specific case referred to by the ratio 1:1, where only one pulse resonates in the cavity at a time. Other multiplicative lengths of the FOPO will also meet the condition of parametric gain. This is accomplished by increasing the FOPO length to any multiple of the oscillator. Such cases are referred to as 1:# of resonant pulses in the FOPO such as; 1:2, 1:10 or 1:100. The reason this can be useful in a fiber based OPO is that this increase in length changes the cavities overall dispersion. The dispersion is a key factor that changes the chirp of the resonant pulse as it propagates, and this plays a large role in the generated spectra and

efficiency. While the current configuration is 1:1, a larger ratio synchronous pumping scheme may be investigated in the future to generated narrower linewidth idler spectra for greater resolution Raman microscopy.
Two different lengths of PCF were also tested, 20cm and 50cm. A few observations were determined from these two different cases. As expected, longer PCF decreased the OPO threshold. What was interesting though is that it did not necessarily increase the conversion efficiency. The major problem found with longer PCF is that, due to the extremely high non-linearity of this fiber, after certain pump powers were reached the spectra became very broad from the signal to the idler. This broadband effect is not desired but higher power is, so the longer PCF became a limiting factor in the desired performance of this system. It is possible that with the desired narrower band pump, this may be less of a problem.

V.IV.IV Characterization

The full generated spectra from the FOPO described above can be seen in Figure 17 a). The spectra correspond to the simulated gain spectra found in the simulations. This confirms OPO operation. The central wavelength of the generated signal and idler was adjusted primarily by tuning the pump wavelength. Some further tunability is accomplished by adjusting the oscillator cavity length (adjusting the specific pump wavelengths synchronously pumped) but this was found to be most useful in fine tuning the shape of the spectra due to the modulation atop of the relatively broad pump. Figure 17 b) & c) show the zoomed-in spectra of the signal and idler respectively. It can be seen from the legend that the linewidth of the signal ranges from 2.5nm to 7.2nm and that of the idler from 4nm to 6.4nm. With the linewidth of the pump from the secondary amplifier being 2.4nm, the Raman response resolution corresponds to 63.37cm^{-1} for the signal and 22.34cm^{-1} for the idler. The idler resolution is within range of current systems, as mentioned previously, further narrowing of spectral linewidth may be achieved. A very impressive characteristic of this system is its wide tunability. The signal was tuned from 779.2nm to 888nm and the idler from 1269.6 to 1507.3nm while still maintaining the desired linewidth. This wavelength tuning with the pump central wavelength corresponds to Raman response tunability from 1686cm^{-1} to 3112cm^{-1} which corresponds to the C-H bond region, silent region and even into the fingerprint region. This tunability is what makes this system capable of Raman excitation for everything from biological samples to remote sensing.

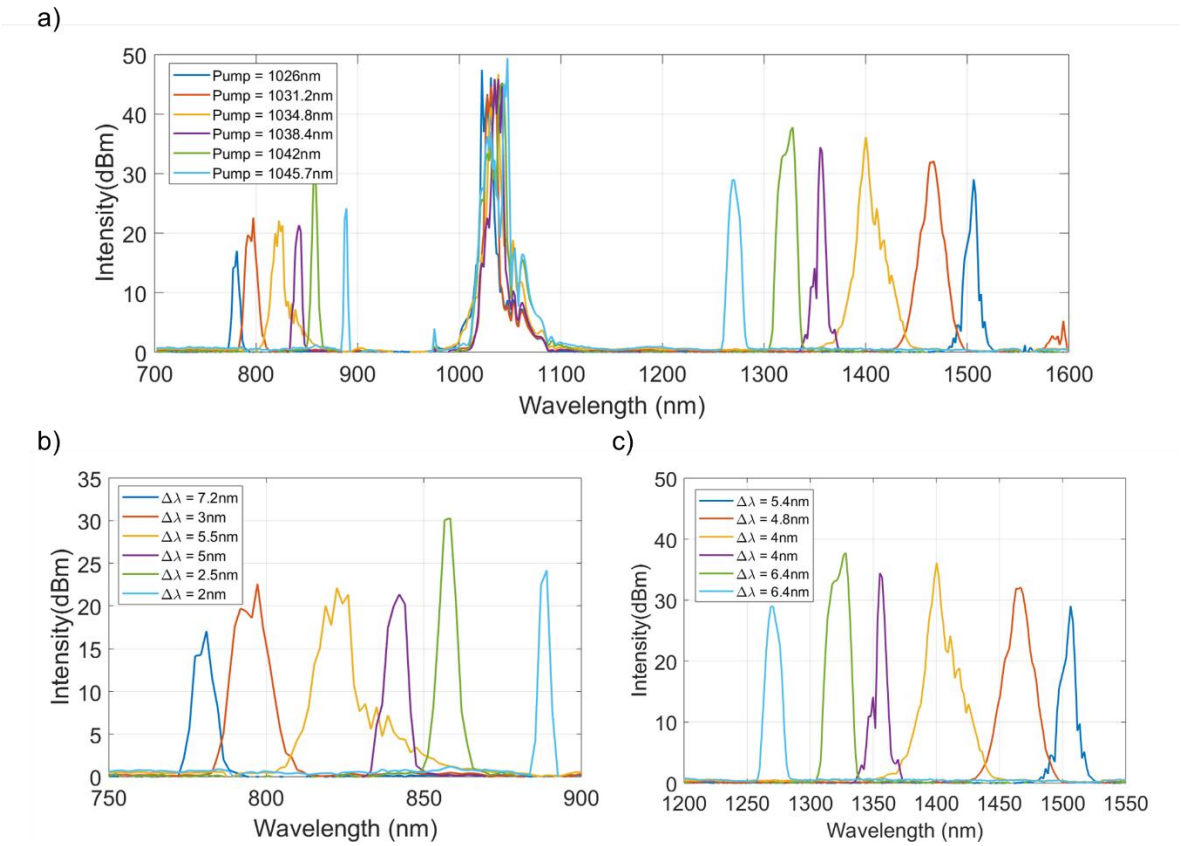

Figure 17: a) Full spectra of the pump, signal and idler generated by tuning the pump wavelength. b) Zoomed in spectra of the generated signal as the pump wavelength was tuned. c) Zoomed in spectra of the generated idler as the pump wavelength was tuned.

The power characteristics of the idler, which will be used in Raman microscopy, are summarized in Figure 18. The output power varies at different idler wavelengths and can be attributed to the phase matching. In general, the output power of the idler is lower than desired for Raman microscopy, less than 20mW even at 1W of pump power. This translates to ~1% conversion efficiency to the idler. It is believed this low conversion efficiency is due to the large spectral linewidth of the pump. Because the power of the pump is distributed over a large linewidth, and the chirp of this system is designed for narrow linewidth, only a portion of the 1W of pump gain is phase matched and converted to the signal and idler.

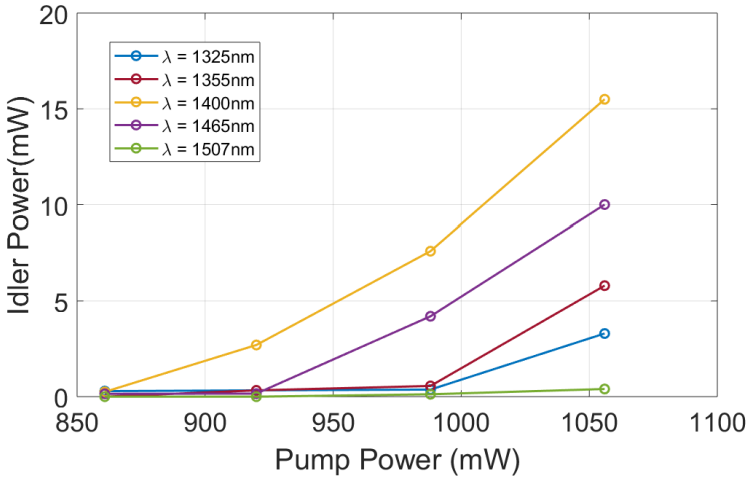

Figure 18: Power curves of Idler at various wavelengths from 1μm pump.

V.VLaser Development Summary

The preceding sections show a successful construction of an all fiber OPO with multiple, relatively narrow band, output wavelengths. The system was constructed in four distinct parts specifically for the purpose of Raman microscopy. An all fiber format was accomplished at a low cost. The very large tuning range demonstrated will enable dynamic Raman microscopy. However, it was pointed out that improvements should be made to improve the linewidth and output power. While measures were taken to reduce SPM (reduction of gain fiber and placement of the amplifier just before the PCF) it is still too large for efficient conversion. The SPM effect is proportional to the intensity of light in the core of the fiber. In order to mitigate this problem, a larger core gain fiber, 20μm will be implemented. We expect this will increase the area by a factor of 4, also reducing the intensity by 4. We expect this will significantly decrease the SPM and increase the parametric conversion efficiency, while simultaneously decreasing the idler linewidth.

VI System Integration for Microscopy

After construction of the laser source, the pump and idler wavelength's must be specially combined and input into the microscope. We intend to investigate both CARS and SRS, and therefore two different integration set ups will be necessary. The following section provides an overview of the all-reflective microscope and discusses the specific tailoring of the input signals for Raman detection.

VI.I Microscope Overview

An all-reflective optical microscope is to be used for this project. The all-reflective nature of this system is important in order to avoid chromatic aberrations since different wavelengths are propagating through the same optics. If refractive elements were used, the final focus points of the signals would occur at different locations and inhibit Raman excitation. This microscope was originally designed for multi-photon microscopy and will be adapted for this laser and application.

Figure 19 shows a schematic of the current microscope. Once the input laser signal is collimated, the beam is expanded by two concave mirrors and one convex mirror. It is then focused down to the sample by an all reflective objective lens. The reflected signal

from the sample is split off by dichroic mirrors and directed to highly-sensitive photo-multiplier tubes (PMT detectors). This general design will be slightly modified both in signal input and detection for Raman microscopy.

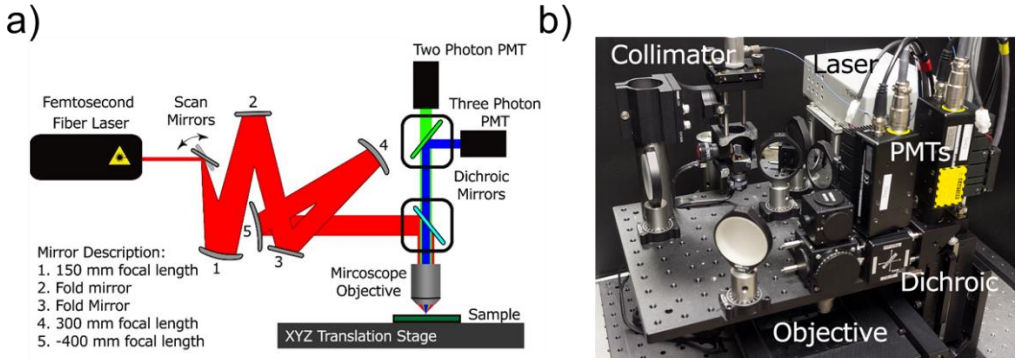

Figure 19: a) Schematic diagram of the current all reflective multi-photon microscope . b) Labeled picture of the all reflective microscope.

VI.II Signal Input

VI.II.I CARS

For CARS microscopy, the two wavelengths from the laser system, pump and idler must first be overlapped in time. This is accomplished by using a home built optical delay stage and additional fiber path length. After the signals are overlapped, the non-PM pump arm is polarized with a λ/2 wave plate and a polarizer to match the polarization of the FOPO idler. A dichroic which passes all wavelengths >1.15μm and reflects all wavelengths below is used to overlap the two wavelengths in space. This combination scheme is constructed with cage components for ease of alignment. The schematic can be seen in Figure 20

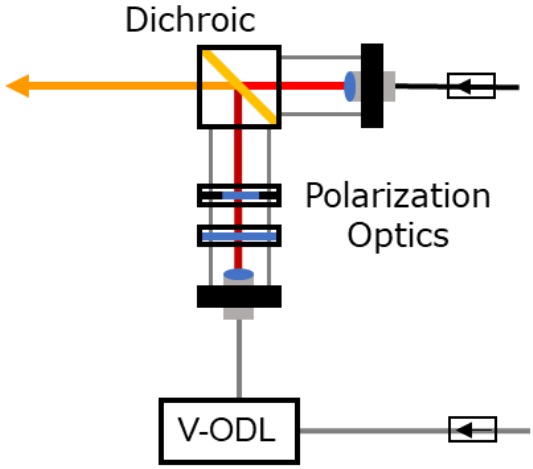

Figure 20: Idler and pump combination for CARS microscopy. This design allows for overlap of the two pulse and matching of their polarizations.

VI.II.II SRS

The signal input scheme for SRS is like that of CARS but unlike CARS, SRS does not produce an anti-stokes signal. Instead of detecting a new generated anti-stokes wavelength, the detection of SRS is dependent on the transfer of an intensity modulation

from the pump to the idler. For this reason, an Acousto-Optic Modulator (AOM) is added to the pump arm for modulation. Figure 21 shows the pump/signal combination schematic used for SRS detection.

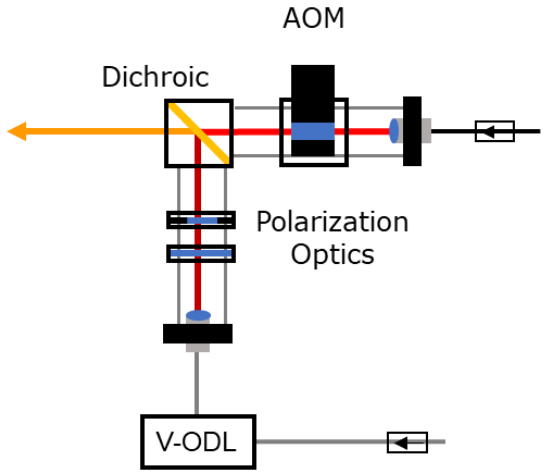

Figure 21: Idler and pump combination for SRS microscopy. This design allows for overlap of the two pulse and matching of their polarizations with the addition of modulation of the pump.

VI.III Detection

Two different detection schemes are set up for CARS and SRS. Like that of the signal integration, CARS is the simpler of the two. This detection scheme does not require much modification of the current multi-photon microscope set-up. The two input wavelengths are focused down and are scanned over the sample by the galvo-mirrors. Because CARS generate a new anti-stokes, blue shifted, wavelength, the current dichroics can be used to split off and detect the reflected Raman Response. When an anti-stokes signal is detected by the PMT's at a specific scanning point, it is amplified then sent to the multi-photon LabView code. This LabView code was written previously by Shai Vardeny for multi-photon detection. It receives this signal from the amplifiers and displays a signal at the corresponding image location.

For SRS, a lock-in amplifier is used to detect the transfer of modulation from the pump to the idler. This electrical device looks for the modulation frequency of the pump in the idler signal and reports its detection to the LabVIEW program. Like before, this signal is displayed at the corresponding image location.

For both CARS and SRS the input laser source is scanned 2/3 dimensionally over the sample to build up and image map of the Raman responses.

VI.IV Laser Tuning

In order to demonstrate the wide Raman excitation capabilities of this laser it is being prepared for imaging of a variety of samples. Traditionally, Poly-methyl methacrylate (PMMA), Polystyrene (PS) and fatty lipids are used as samples. The molecular bonds of these samples correspond to 2840cm^{-1}, 2950cm^{-1} and 3050cm^{-1} respectively. As mentioned previously, by tuning the difference of this laser systems pump and idler arms these Raman responses can be excited. Figure 22 demonstrates the spectral capability of this laser system to detect these specific molecules.

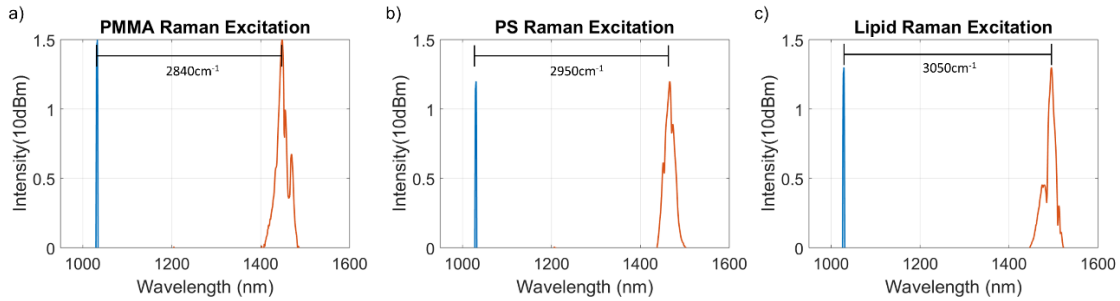

Figure 22: Overlaid idler and secondary pump spectra of laser system used to excite the Raman response of PMMA, PS and Lipids.

VII Directed Energy Applications

Directed energy is a field of electro-magnetic (EM) technology centered around propagation of directed EM radiation down range primarily for Department of Defense purposes. This field encompasses many laser and microwave technologies and one of significant important is that of remote sensing. Remote sensing utilizes directed radiation sources to obtain information about a situation at significant distances away from the source.

Many different laser technologies are used to do this, specifically laser spectroscopy techniques. Lasers allow the ability to send directed optical signals at long ranges with enough reflected energy to return information while spectroscopy is a science that allows information to be gathered about the chemical make-up of a sample area. The fingerprint spectral region comprises molecules associate with explosives and chemical weapons. For this reason, this spectral region is important for remote sensing. While multiple laser spectroscopy techniques are currently used for such, one that has not been explored as thoroughly for remote sensing is that of laser Raman spectroscopy.

Mid-IR frequency combs, Fourier Transform Infrared Spectroscopy (FTIR) and supercontinuum source spectroscopy are all techniques currently used to determine the presence of such chemicals in the fingerprint region. These techniques can be accomplished in many ways and have significant merits though common downsides to all of these techniques are complexity and underdevelopment. There are well developed Raman laser sources such as the Ti:S and locked Ytterbium laser system mentioned previously which could possibly be used for such applications though this type of system also suffers from inefficiency and complexity. The system described in this thesis demonstrates a developed, relatively simple, all fiber laser source that can operate in the Visible/NIR atmospheric transmission window.

While this FOPO laser system was developed for biological applications, its broad tunability into the fingerprint region shows promise in remote sensing directed energy applications. The fact is that an ultra-fast laser constructed in an all-fiber format provides promise for the military's Size Weight And Power (SWAP) requirements. The proposed schematic of our all fiber Raman excitation/detection source utilized for remote sensing is described in Figure 23.

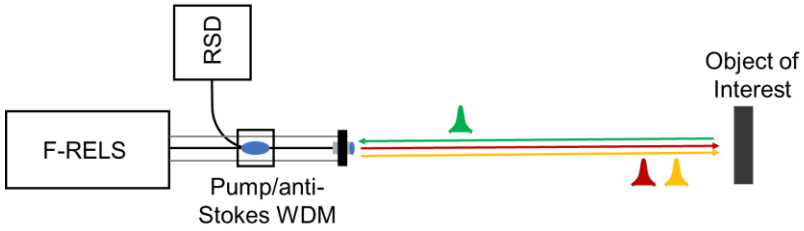

Figure 23: Proposed schematic description of our all fiber Raman excitation/detection source utilized for remote sensing.

VIII Conclusion

Raman microscopy is an extremely important and versatile tool for the identification of a variety of molecules in microscope samples. It offers capabilities not possible in standard microscopes or even multi-photon microscopes. The development of the laser source described in this thesis marks a milestone for advancing this technique by dramatically reducing cost and complexity with this novel laser architecture. Additionally, good resolution was maintained and tuning capabilities were increased compared to current systems. There are a few modifications that are necessary to further increase the performance, but the initial results give us confidence in the capabilities of this system.

IX References

[1] "Pancreatic cancer cell detection by targeted lipid microbubbles and multiphoton imaging." [Online]. Available: https://www.spiedigitallibrary.org/journals/Journal-of-Biomedical-Optics/volume-23/issue-4/046501/Pancreatic-cancer-cell-detection-by-targeted-lipid-microbubbles-and-multiphoton/10.1117/1.JBO.23.4.046501.full?SSO=1. [Accessed: 10-Jun-2019].

[2] B. Cromey, R. J. Knox, and K. Kieu, "3D imaging of gems and minerals by multiphoton microscopy," *Opt. Mater. Express*, vol. 9, no. 2, p. 516, Feb. 2019.

[3] "Raman scattering," *Wikipedia*. 15-Apr-2019.

[4] A. M. Hanninen, R. C. Prince, and E. O. Potma, "Triple Modal Coherent Nonlinear Imaging With Vibrational Contrast," *IEEE J. Sel. Top. Quantum Electron.*, vol. 25, no. 1, pp. 1–11, Jan. 2019.

[5] K. Kieu, B. G. Saar, G. R. Holtom, X. S. Xie, and F. W. Wise, "High-power picosecond fiber source for coherent Raman microscopy," *Opt. Lett.*, vol. 34, no. 13, p. 2051, Jul. 2009.

[6] I. Rocha-Mendoza, W. Langbein, and P. Borri, "Coherent anti-Stokes Raman microspectroscopy using spectral focusing with glass dispersion," *Appl. Phys. Lett.*, vol. 93, no. 20, p. 201103, Nov. 2008.

[7] Y. Ozeki, T. Asai, J. Shou, and H. Yoshimi, "Multicolor Stimulated Raman Scattering Microscopy With Fast Wavelength-Tunable Yb Fiber Laser," *IEEE J. Sel. Top. Quantum Electron.*, vol. 25, no. 1, pp. 1–11, Jan. 2019.

[8] Y. Ozeki *et al.*, "High-speed molecular spectral imaging of tissue with stimulated Raman scattering," *Nat. Photonics*, vol. 6, no. 12, pp. 845–851, Dec. 2012.

[9] E. S. Lamb, S. Lefrancois, M. Ji, W. J. Wadsworth, X. S. Xie, and F. W. Wise, "Fiber optical parametric oscillator for coherent anti-Stokes Raman scattering microscopy," *Opt. Lett.*, vol. 38, no. 20, pp. 4154–4157, Oct. 2013.

[10] S. Lefrancois *et al.*, "Fiber four-wave mixing source for coherent anti-Stokes Raman scattering microscopy," *Opt. Lett.*, vol. 37, no. 10, pp. 1652–1654, May 2012.

[11] T. Gottschall *et al.*, "Fiber-based optical parametric oscillator for high resolution coherent anti-Stokes Raman scattering (CARS) microscopy," *Opt. Express*, vol. 22, no. 18, p. 21921, Sep. 2014.

[12] "RP Photonics Encyclopedia - parametric nonlinearities." [Online]. Available: https://www.rp-photonics.com/parametric_nonlinearities.html. [Accessed: 02-May-2019].

[13] R. W. Boyd, *Nonlinear Optics*. Elsevier, 2003.

[14] E. A. Zlobina, S. I. Kablukov, and S. A. Babin, "Tunable CW all-fiber optical parametric oscillator operating below 1 μm," *Opt. Express*, vol. 21, no. 6, pp. 6777–6782, 2013.